J. Fluid Mech. (1981), *vol.* 105, *pp.* 451-467
Printed in Great Britain

The turbulent trailing vortex during roll-up

By W. R. C. PHILLIPS
Department of Engineering, University of Cambridge†

(Received 16 February 1978 and in revised form 11 August 1980)

The turbulent trailing vortex forming from a rolling-up vortex sheet is considered. The inviscid, asymptotic roll-up of a vortex sheet is briefly reviewed, as are the effects to the sheet of merging by viscous and turbulent diffusion. The merged region is found to rapidly attain a state of equilibrium and similarity variables are used to describe it. The detailed distributions of circulation and Reynolds stress are seen to depend to some extent upon the initial spanwise distribution of circulation on the wing. However, a tiny region which is independent of the wing circulation distribution is found to exist near the point of peak tangential velocity. It is suggested that this region is described by Hoffmann & Joubert's logarithmic relationship. Assuming this to be the limiting form for the distribution of circulation near r_1, the radius where the tangential velocity takes its peak value v_1, an approximate form for the distribution of circulation is found and this is used to determine the form of the Reynolds-stress distribution. It is found that two modes for the decay of v_1 with time are possible: one when r_1 is much less than $\frac{1}{2}s$, the wing semi-span, and v_1 decays like $t^{-\frac{1}{2}n}$; and the other when $r_1 = O(\frac{1}{2}s)$ and v_1 may decay like $t^{\frac{1}{2}(n-2)}$; $0 < n < 1$, for elliptic wing loading $n \simeq \frac{1}{2}$.

1. Introduction

Streamwise vorticity is generated whenever a finite wing produces lift and sheds from the wing to form a continuous vortex sheet. The velocity field due to the sheet may vary in the spanwise direction and wherever this field is singular along the sheet it is likely to roll up into a spiral with a continuously increasing number of turns. The innermost turns of this spiral become almost circular and the distance between each turn small enough so that diffusion blurs the discrete spiral structure and makes the distribution of vorticity a smooth one. We call this merged region within the spiral structure a trailing vortex. Furthermore, we consider the trailing vortex to be undergoing roll-up so long as it remains surrounded by discrete arms of the spiralled vortex sheet; only when irrotational fluid completely surrounds the merged region is the trailing vortex fully rolled up.

Dynamics require axial velocities to be present in trailing vortices (Batchelor 1964) and these can have an important effect on the stability of the trailing vortex system and play an important role in the occurrence of vortex breakdown (Widnall 1975; Leibovich 1978). But the persistence of trailing vortices behind lightly loaded wings suggests that considerable time is required before instabilities are excited and in the interim period, and until the vortices finally dissipate, those trailing from jumbo jets for example, can pose a hazard to smaller following aircraft. It is concern for this hazard that has prompted recent interest in trailing vortices.

Measurements in vortices behind lightly loaded wings indicate that very close to

† Presently, National University of Singapore, Kent Ridge, Singapore 0511

the wing the peak axial velocity perturbation, u_1 say, is roughly equal to the peak tangential velocity v_1 (see Fage & Simmons 1925; Hilton 1938; Mason & Marchman 1972). And as v_1 (with light loading) is much less than the free-stream velocity U_∞, so too is u_1. Under these conditions the equations of motion may be linearized and this has formed the basis of many papers concerning laminar and, with some *ad hoc* closure procedure, turbulent trailing vortices (Batchelor 1964; Squire 1965; Govindaraju & Saffman 1971; Saffman 1973; and others). These papers also assume that the vortices are fully rolled up.

But vortex sheets roll up asymptotically and it may be many wing spans behind the aircraft before the fully rolled-up condition is reached. We should like to have clear ideas about the behaviour of the trailing vortex system during the roll-up period and this prompted the work of Moore & Saffman (1973). These authors considered the trailing vortices forming behind a lightly loaded wing on which the boundary layer is laminar. But, with the high Reynolds numbers encountered on lifting wings in free flight, it is likely that their boundary layers, and thus their trailing vortex sheets, are turbulent. In the present article, therefore, we consider the trailing vortices undergoing roll-up behind a lightly loaded finite wing on which the boundary layer is turbulent. We begin (in §2) with a brief review of inviscid roll-up and in §3 consider the merging process. We note that the merged region rapidly attains a state of equilibrium and in §4 use similarity variables to describe it. The apparent dependence of trailing vortices on Reynolds number is discussed in §5 and in §6 we consider the possibility that trailing vortices have two modes of decay.

2. Inviscid roll-up

The initial strength of a vortex sheet is specified by the spanwise distribution of lift on the wing from which it sheds and we should like to determine the detailed motion of a trace of this sheet with time t, for $t > 0$, in the downstream plane $z = U_\infty t$.

If the vortex sheet is semi-infinite, has a circulation distribution which decreases monotonically toward one edge and contains a velocity-field singularity there, then the sheet will roll up into a continuous spiral. Furthermore, the trace of the spiral which forms (when viewed in any downstream plane) is self-similar and the radial distribution of circulation in the ever tightening innermost part of the spiral is asymptotic to the distribution on the originally planar sheet, but with the distance from the sheet edge x replaced by $\alpha_n r$, where r is the radius from the spiral centre and α_n is the Betz constant. This feature was first realized by Kaden (1931) and is well supported by numerical solutions of Kaden's problem (see Pullin & Phillips 1981).

To determine the motion of a finite vortex sheet with the same properties as above is more difficult; however Moore (1974) and Fink & Soh (1978) have obtained numerical solutions for the case of an initially planar elliptically loaded sheet. Moore compares the roll-up rate of this sheet with that given by Kaden's similarity analysis (for a parabolically loaded sheet) and finds that the two agree until about 50 % if the sheet's vorticity is contained within the rolled-up spiral; after this Kaden's result gradually starts to over-predict the roll-up rate. Thus, during the initial stages of roll-up behind a finite wing, it would seem reasonable to utilize the simple ideas of Kaden to describe the outer inviscid flow field of a trailing vortex.

This was done by Moore & Saffman, who considered the vortices forming behind a

wing of span s. Assuming the wing-tip loading to be $2\Gamma_\infty(s/x)^{n-1}$ $(0 < n < 1)$, where Γ_∞ is the root circulation, the asymptotic form of the innermost spiral of the rolling up trailing vortex sheet is then

$$r = (\zeta t/\theta)^{1/(1+n)}, \tag{2.1}$$

where $\zeta = (\Gamma_\infty/\pi)(s/\alpha_n)^{n-1}$ and θ is the angular co-ordinate. And, as $\theta \to \infty$, and it becomes a good approximation to replace the discontinuous vorticity field with a smoothed one, the tangential velocity is given by

$$v_\theta \simeq \zeta/r^n. \tag{2.2}$$

3. The merged region

3.1. *Diffusive merging*

At finite Reynolds numbers, vorticity diffuses, and the sheet becomes a vortex layer of finite, non-zero thickness. Successive turns in the centremost portions of the rolled-up layer merge, the spiral structure disappears and, if the radius of the vortex core is much greater than the diffusive length scale, an equilibrium structure ensues (Maskell 1962).

Thus, we might anticipate a multi-structured core, the innermost part of which has effectively reached a state of equilibrium and surrounding this an annulus in which the turns have merged or are in various stages of merging, and an outer region, beyond a radius a_0 say, in which discrete turns of the spiral remain evident.

3.2. *Limit of the smoothed-out region*

Now if $l(t)$ is the layer thickness at time t, then we might expect turbulent diffusion to have a length scale of $O(l)$; while laminar diffusion has a length scale of $O[(\nu t)^{\frac{1}{2}}]$. Moreover, in the early stages of roll-up, the thickness of the layer should be $O(\delta)$, where δ is the boundary-layer thickness at the wing trailing edge. So at this stage, if $\delta \gg (\nu t^{\frac{1}{2}})$, it is reasonable to expect diffusion in the region of a_0 to be predominantly turbulent. But as the sheet rolls up it is stretched laterally and l decreases, so some time later, when $l \ll (\nu t)^{\frac{1}{2}}$, diffusion should be predominantly viscous.

The approximate distance between successive turns follows from (2.1) and, if we require this to be small compared with the diffusive length scale, we find that, for laminar diffusion, the assumption of a smoothed-out vorticity distribution is valid provided $r \ll [\gamma\nu^{\frac{1}{2}}t^{\frac{3}{2}}]^{1/(n+2)} = a_v$ say; and for turbulent diffusion $r \ll [\gamma t l]^{1/(n+2)} = a_t$ say, where $\gamma = (n+1)\zeta/2\pi$. Clearly the radius a_0, which from (2.1) is proportional to $[\zeta t]^{1/(n+1)}$, must be greater than both a_t and a_v. Moore & Saffman require that a_0 be effectively infinite compared with the radius of the viscous core $(= O[(\nu t)^{\frac{1}{2}}])$, so for consistency we choose a_0 to be effectively infinite compared with δ; a_0 is then greater than a_v and a_t if $t \gg \delta^{1+n}/\zeta$.

3.3. *The behaviour of* $\overline{v_r' v_\theta'}$ *as* $r \to a_0$

The growth of a_0 is explained physically as the continuous addition of turns to the merged vortex core. It is through this process that angular momentum, confined initially to the rolling-up vortex layer, is added to the merged core. This radial transport of angular momentum is equivalent to a torque, and, providing no external torque is applied to the boundary, the change in angular momentum of the fluid within a circle of radius r say (which varies with time), i.e.

$$\rho \frac{\partial}{\partial t} \int_0^{2\pi} \int_0^{r(t)} r^2 v_\theta \, dr \, d\theta,$$

is equal to the flux of angular momentum entering the circle,

$$-\rho\int_0^{2\pi} r^2(v_r v_\theta + \overline{v_r' v_\theta'} - v_\theta\, da_0/dt)\, d\theta.$$

Since $v_r = 0$, there is no transfer of mass into a circle of fixed radius and no associated flux of angular momentum. But as the vortex layer, and subsequently the merged vortex, is turbulent, neither v_r' nor v_θ' are zero (except at random points in time) and the pertinent question is: can these fluctuations in velocity lead to a flux of angular momentum into a circle of fixed radius? We note that with zero flux of angular momentum Saffman's overcirculation theorem† must apply. This theorem clearly applies to a fully rolled-up vortex where the outer flow field is irrotational, but in the present case the outer flow field is *rotational*.

Now if we consider this rotational field to be composed of many vortex lines, it follows that a small movement in position of any particular vortex line, relative to the others, must change the local induced velocity field and, moreover, the simultaneous fluctuations about the mean positions of a multitude of vortex lines, due to turbulent motions, must inevitably affect the instantaneous induced velocity field. So it would seem most unlikely, in circumstances such as these, that v_r' and v_θ' are uncorrelated. This means that random fluctuations in the radial and tangential velocities can lead to a flux of angular momentum (albeit small), with no net transfer of mass, across a circle of fixed radius. That is, as $r \to a_0$,

$$-\frac{1}{2\pi}\int_0^{2\pi} r^2 \overline{v_r' v_\theta'}\, d\theta = \vartheta,$$

where ϑ is small but not zero. Further, to be consistent with the inviscid velocity field in which this flux is acting, we should expect ϑ to be independent of time (at least to leading order). With this premise, overcirculation is extremely unlikely during the roll-up process; see appendix.

3.4. *Three regions within the merged core*

It is desirable at this point to divide the merged core into three regions (see figure 1):

(i) The innermost part we denote region I, and in this region viscous effects must be present to bring the tangential velocity to zero on $r = 0$. Moreover, near $r = 0$, the rotation is close to solid-body (i.e. $v_\theta(r, t) = r\Omega(t)$, where $\Omega(t)$ is the angular velocity); and to leading order $-r^2\overline{v_r' v_\theta'} = \frac{1}{4}r^4\, d\Omega/dt$ $(r \to 0)$, so the shear stress $\rho\overline{v_r' v_\theta'}$ is evidently positive and increasing (assuming $d\Omega/dt < 0$, which is physically plausible).

(ii) In region II viscous effects are likely to be small. The tangential velocity reaches a maximum at a radius r_1 and then decreases. And from considerations of the transfer of tangential velocities by the random radial motions of small parcels of fluid, we may deduce that $\rho\overline{v_r' v_\theta'}$ should change sign at some point close to, but not necessarily at, r_1; we should also expect $\rho\overline{v_r' v_\theta'} > 0$ for $r < r_1$.

Now near r_1, Hoffmann & Joubert's (1963) logarithmic law for circulation applies. Defining $\Gamma_1 = 2\pi v_1 r_1$, we may express this as

$$K = \frac{\Gamma}{\Gamma_1} = \ln\left(\frac{r}{r_1}\right) + 1 \quad (r \to r_1). \tag{3.1}$$

† This theorem states that overcirculation, i.e. $\Gamma > \Gamma_\infty$, will be in evidence at some stage during the development of the vortex; see appendix.

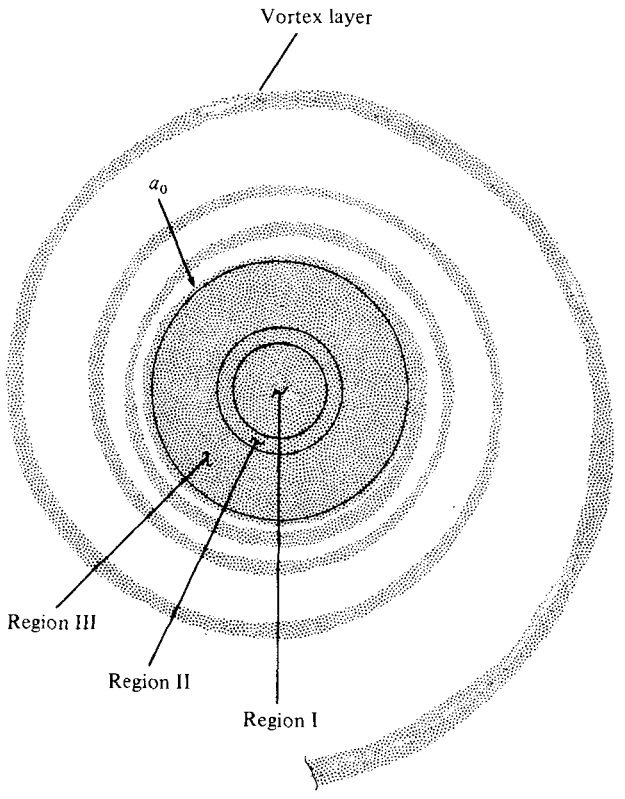

FIGURE 1. Sketch of roll-up and merging of a trailing vortex layer.

There appears to be no rigorous derivation for (3.1) but experimental data follow it closely. In figure 2 we plot the data of Graham, Newman & Phillips (1974) in the co-ordinate system suggested by (3.1). The data is for their cases B, C and D (measured in zero pressure gradient in a turbulent vortex generated by two half-wings in a circular blower tunnel): in case B a jet is superimposed on the vortex axis ($u_1/v_1 \simeq 1$); case C is almost planar ($u_1/v_1 \simeq 0$); and, in case D, a wake is superimposed ($u_1/v_1 \simeq -1$). It is clear that (3.1) is well supported for much of the core ($0{\cdot}9 < r/r_1 < 2$) both with and without axial velocities present. This is not to say that (3.1) actually describes the data over all of region II but that the data fall close to (3.1); we shall return to this point in §4.4.

(iii) In region III the closely spaced turns of the spiral have merged, or are in the process of merging, by diffusion (both viscous and turbulent). Since the Reynolds number (Γ_∞/ν) is very high, we have assumed that the merging process has served simply to smooth out the discontinuities in the inviscid velocity distribution, while leaving its overall form unaltered from (2.2). In this region, $\rho\overline{v_r'v_\theta'}$ tends to zero like the inverse square of radius, presumably from below; see §3.3.

Now we should expect a gradual change from one region to the next, but for the purpose of analysis it is desirable to treat the three regions separately. We therefore assume an interface of radius r_i separating regions I and II, and an interface of radius r_s separating regions II and III. We attempt to define these radii in §4.

4. Analysis of the merged region

4.1. *Formulation and solution*

In analysing the region bounded by a_0, we assume that the viscous stresses within region I are effectively confined to a region of radius $O(\nu t)^{\frac{1}{2}} < r_1$ and that the axial velocity perturbation, while dynamically necessary, is small compared with U_∞. The fluid is incompressible.

Consider then a set of polar co-ordinates (r, θ, z) where the origin O is the vortex axis, r is the radius from the axis and z is the distance downstream of the wing. The velocity components are then v_r, v_θ and $U_\infty + v_z$ in the r, θ and z directions respectively. Within the bounds of the light-loading approximation, $v_z/U_\infty \ll 1$, we can examine the core region of the vortex using approximations of the boundary-layer type. So, assuming axial symmetry of the vortex core, and taking a reference frame moving with U_∞, we may write the tangential momentum equation as

$$\frac{1}{2\pi}\frac{\partial \Gamma}{\partial t} = \nu \frac{1}{2\pi r}\frac{\partial}{\partial r}\left[r^3 \frac{\partial}{\partial r}\left(\frac{\Gamma}{r^2}\right)\right] - \frac{1}{r}\frac{\partial}{\partial r}(r^2 \overline{v_r' v_\theta'}). \tag{4.1}$$

The boundary conditions for the vortex core are that, at $r = 0$, $v_\theta = 0$ and $\overline{v_r' v_\theta'} = 0$; and, as $r/r_1 \to \infty$, v_θ and $\overline{v_r' v_\theta'}$ should match with the limiting form of the inviscid solution. That is,

$$v_\theta \sim \frac{\zeta}{r^n} \quad \text{and} \quad \overline{v_r' v_\theta'} \sim -\frac{\vartheta}{r^2} \quad (r \to \infty). \tag{4.2}$$

As equation (4.1) is parabolic, we require initial conditions on v_θ and $\overline{v_r' v_\theta'}$. Consistent with the boundary-layer approximation, we obtain these by assuming that (4.2) holds at $t = 0$, so that

$$v_\theta(r, 0) = \frac{\zeta}{r^n} \quad \text{and} \quad \overline{v_r' v_\theta'}(r, 0) = -\frac{\vartheta}{r^2}.$$

We seek a solution to (4.1) by the method of separation of variables. Introducing the non-dimensional variable $\eta = (r/r_1(t))^2 \, (0 \leqslant \eta \leqslant \infty)$ and the dimensionless functions $\Phi(\eta)$ and $G(\eta)$, which represent the vorticity and Reynolds stress respectively, we write

$$\Gamma(\eta, t) = H(t) \int_\eta \Phi(\eta) \, d\eta \tag{4.3}$$

and

$$\overline{v_r' v_\theta'}(\eta, t) = \Theta(t) \, G(\eta), \tag{4.4}$$

where $H(t)$ is a function to be defined and $\Theta(t) = \nu H(t)/\pi r_1^2(t)$. Further, writing $\eta = -2\beta/A_2$, we may express (4.1) as

$$\frac{d^2\Phi}{d\beta^2} + \frac{d\Phi}{d\beta}\left(\frac{1}{\beta} - 1\right) - \frac{\Phi}{\beta}\left(\frac{2A_2 - A_1}{2A_2}\right) = \frac{1}{\beta}\frac{d^2}{d\beta^2}(\beta G), \tag{4.5}$$

where

$$A_1 = \frac{r_1^2(t)}{\nu H(t)} \frac{dH}{dt} \tag{4.6}$$

and

$$A_2 = \frac{r_1(t)}{\nu} \frac{dr_1}{dt}. \tag{4.7}$$

For self-preserving flow A_1 and A_2 are constants.

The general solution of equation (4.5) follows once we define a particular integral Φ^J of (4.5). First, noting that the leading term in $G(\beta)$ goes like β^{-1} as $\beta \to -\infty$, the asymptotics of (4.5) show that

$$\Phi^J(\beta) \sim \Lambda(-\beta)^{(A_1-2A_2)/2A_2} \quad \text{as} \quad \beta \to -\infty,$$

where Λ is a constant provisionally unknown. Second, since the differential equation has a regular singular point at $\beta = 0$, if we require $\Phi^J(0) = 0$, the function $\Phi^J(\beta)$ is uniquely defined.

Now from the physics of the problem, the boundary and initial conditions require that

$$\Phi(\beta) \sim \tfrac{1}{2}(1-n)\,Q(-\beta)^{\frac{1}{2}(-1-n)} \quad \text{as} \quad \beta \to -\infty, \tag{4.8}$$

where Q is a constant readily found from (2.2) and

$$\Phi(\beta) \simeq \frac{2\pi\Omega(t)\,r_1^2(t)}{H(t)} = \phi_0 \quad \text{as} \quad \beta \to 0.$$

Further from (4.5)

$$\Phi(\beta) \sim J(-\beta)^{(A_1-2A_2)/2A_2} \quad \text{as} \quad \beta \to -\infty. \tag{4.9}$$

So, comparing (4.8) with (4.9), we require that

$$A_1/A_2 = 1-n \tag{4.10}$$

and $J = \frac{1}{2}(1-n)\,Q$. We must now choose Λ such that

$$\Lambda = \tfrac{1}{2}(1-n)\,Q - \frac{\phi_0}{\Gamma(\frac{1}{2}(1-n))},$$

where $\Gamma(\frac{1}{2}(1-n))$ is the gamma function.

We have implicitly assumed in (4.10) that both A_1 and A_2 are positive: their sign does not affect the mathematics but has physical implications regarding the vortex growth rates, and we shall discuss this in § 6. The general solution may now be written as

$$\Phi_n(\beta) = \Phi_n^J(\beta) + \phi_0\,{}_1F_1(\tfrac{1}{2}(n+1); 1; \beta), \tag{4.11}$$

where ${}_1F_1$ is a confluent hypergeometric function of the first kind (Slater 1960). We shall discuss equation (4.11) in § 4.3 and in § 4.7 we determine Φ_n^J.

4.2. *The vortex growth rates*

As both A_1 and A_2 are constant, equations (4.6) and (4.7) are readily integrable, giving

$$r_1^2(t) = 2\nu A_2 t \tag{4.12}$$

and

$$H(t) \propto t^{\frac{1}{2}(1-n)}. \tag{4.13}$$

And, as it can be shown that $\Gamma_1(t) = N[2\nu A_2 t]^{\frac{1}{2}(1-n)}$ (N = constant), it is clear that $H(t)$ is proportional to $\Gamma_1(t)$. Moreover, with no loss of generality, we can take the constant of proportionality to be unity.

4.3. *Discussion of theory and experiment*

Although Φ_n^J is unknown, we can still deduce the overall behaviour of (4.11). First, it is likely to be dependent upon the value of n; this is reasonable in view of the fact

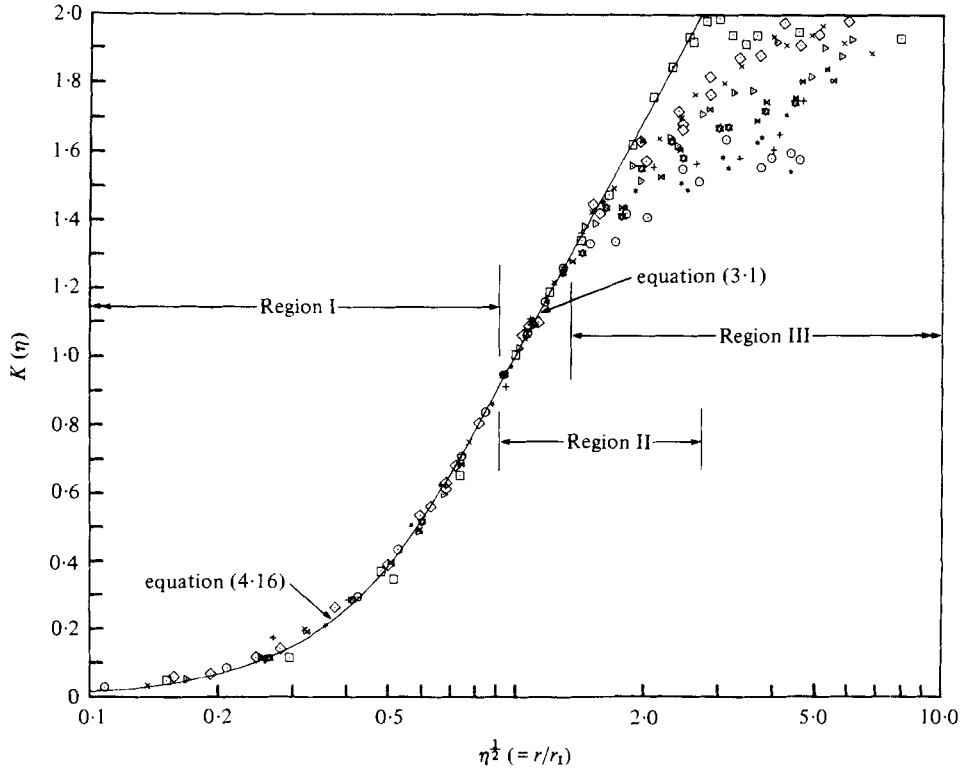

FIGURE 2. Distribution of $K(\eta)$ in the turbulent trailing vortex. Data of Graham *et al.* (1974) in sequence (see text) *B*, *C*, *D*: *, +, ⊡, $z/c = 45$; ⊙, ▷, ◇, $z/c = 78$; ✡, ⋈, ×, $z/c = 109$.

that the outer boundary condition on the tangential velocity is n dependent, and in light of this we might expect a family of similarity curves, each representative of a different value of n. Moreover, the similarity solution should embrace all of regions I, II and III, and should reproduce (in somewhat more detail) the behaviour we anticipated for each.

The experimental data for $K(\eta)$† differs on two counts however: first, only one curve is apparent through the collapsed data and, second, collapse is only evident in regions I and II.

The first is consistent, because the wing loading in all the experimental cases (in figure 2) was effectively constant with $n \simeq \frac{3}{4}$. But the data in region III should also collapse about one curve and from figure 2 this does not appear to be the case.

Now, although the measurements given in figure 2 were taken in vortices shed from same wing, the initial conditions under which they shed differ (because of an imposed axial velocity perturbation, see § 3.4). And while velocity perturbations in the axial direction do not appear to affect the similarity form reached by the vortex – at least for $v_z/U_\infty \ll 1$ – it apparently does affect the rate with which the vortex attains this form. This is suggested in figure 4: for if we consider figure 4(*a*), which shows the case for $u_1/v_1 \simeq 0$ at three downstream stations, we see that the data collapse in regions I

† The data are plotted in figure 2 as $K(\eta) = \Gamma(\eta, t)/\Gamma_1(t)$ and, as we can see from (4.3), $K(\eta) = \int_\eta \Phi(\eta)\, d\eta$.

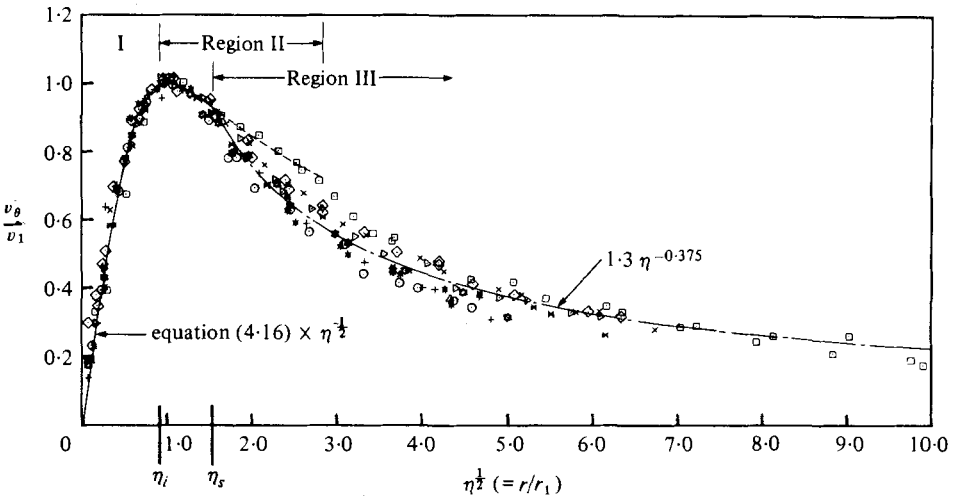

FIGURE 3. Non-dimensional tangential velocity distribution in trailing vortex. Data of Graham *et al.*; symbols as in figure 2.

and II, but in region III, appear to be tending toward collapse only at large $\eta(\simeq 25)$. In figure 4(*b*) however (which shows the corresponding data for a vortex within which $u_1/v_1 \simeq -2$) the data does collapse over the three regions, and it seems reasonable to suggest that in this case the vortex has reached its complete similarity form.

Now the physical development towards this form is reached in two stages: one is the merging of the spiral turns near a_0 and the other is the development and expansion of the inner equilibrium region. So, between these two regions that have reached their equilibrium state, lies an annulus of fluid still in the process of finding equilibrium. Thus, if we consider figure 4(*c*), we might expect the final stages of the progression to the complete similarity form to be much like that indicated by the dotted curves, the final form being a solid curve, and this behaviour is consistent with the available data.

4.4. *Form of the solution near* $\eta = 1$: *region II*

Now (4.11) implies a family of similarity curves but we must note that in the vicinity of $\eta = 1$ there is a region (although its extent is probably small) through which all of these curves overlap. This follows from the constraints on $K(\eta)$ at $\eta = 1$, viz. that $K(1) = 1$ and $dK/d\eta = \frac{1}{2}$. Thus, as the solution for $K(\eta)$ in this tiny region is independent of both n and a_0, the region is truly *universal*.

The logarithmic law satisfies both constraints at $\eta = 1$ (see (3.1)) and, according to Hoffmann & Joubert, it is universal. But, if the log law is a true description of the solution for $K(\eta)$ at $\eta = 1$, we must think of it only as the *limiting form* for $K(\eta)$ in the vicinity of $\eta = 1$, to which each of the similarity solutions asymptotes, rather than the actual solution for the whole of what we have called region II. The scatter in experimental data overshadows this point and lead to the reasonable, but mistaken, impression that the logarithmic law describes a much larger region of the vortex core than in fact it does. In view of this, we now redefine region II to be the region in which $K(\eta)$ is within (say) 1% of that described by the log law. Furthermore, we may exploit the known behaviour of $K(\eta)$ near $\eta = 1$ to help determine approximate solutions for $K(\eta)$ in regions I and III.

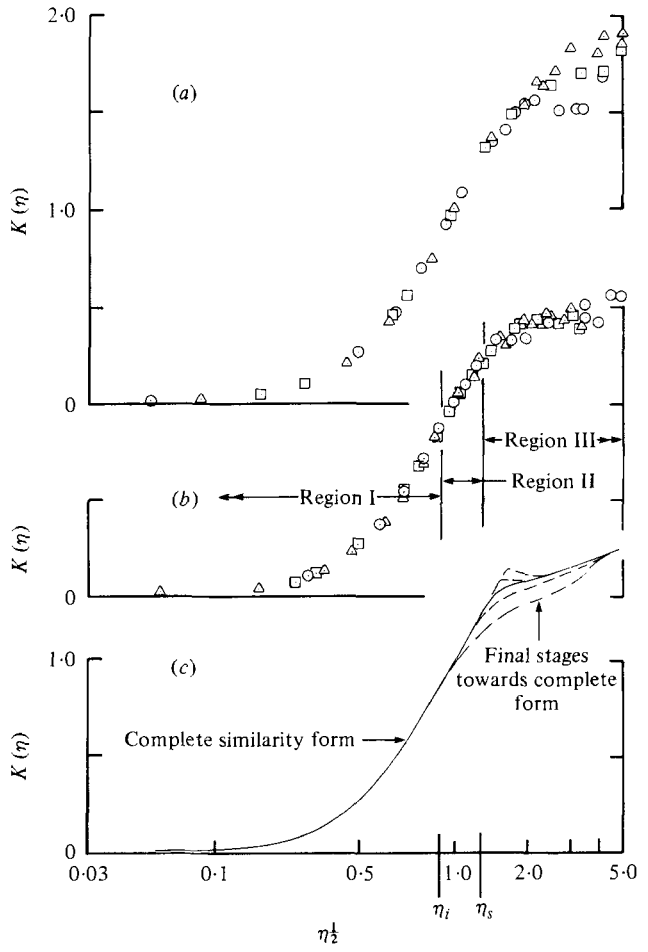

FIGURE 4. Progression toward the complete similarity form. Data of Graham *et al.*: ○, $z/c = 45$; □, $z/c = 78$; △, $z/c = 109$. (*a*) $u_1/v_1 \simeq 0$, (*b*) $u_1/v_1 \simeq -2$.

4.5 *Region I*

As the series form of (4.11) is known, we may write†

$$K(\eta) = \phi_0\eta - \phi_1\eta^2 + \phi_2\eta^3 - \ldots, \tag{4.14}$$

where ϕ_1 and ϕ_2 are constants which, we presume, are dependent in some way upon n. And, as circulation increases almost logarithmically with radius near $\eta = 1$, we state

$$K(\eta) \sim \tfrac{1}{2}\ln(e^2\eta) \quad (\eta \to 1). \tag{4.15}$$

Our aim is to match (4.14) to (4.15) at $\eta = \eta_i$.

Ideally, this would imply that both K^{I} and K^{II} are continuously differentiable at $\eta = \eta_i$. But the only function, defined in $0 < \eta < \eta_i$, that satisfies this condition, is the analytic continuation of $\frac{1}{2}\ln(e^2\eta)$, and to force this to be finite at $K^{\mathrm{I}}(0)$ leads to non-unique coefficients.

† This follows from the complementary function

$$\phi_0\,{}_1F_1\left(\frac{n+1}{2}; 1; \beta\right) = \phi_0\left[1 + \left(\frac{n+1}{2}\right)\beta + \frac{(n+1)(n+3)}{16}\beta^2 + \ldots\right].$$

We choose a solution for region I, therefore, that is differentiable only so far as is necessary to satisfy the more important physical properties at $\eta = \eta_i$, that is, we match the circulation, vorticity, gradient of vorticity and gradient of the gradient of vorticity at the interface. This permits us to solve for η_i and the first three coefficients of ϕ_j ($j = 0, 1, \ldots$). We write then

$$K^{\mathrm{I}}(\eta) = \phi_0\eta - \phi_1\eta^2 + \phi_2\eta^3, \tag{4.16}$$

and find that the coefficients are

$$\phi_0 = 1{\cdot}7720, \quad \phi_1 = 1{\cdot}0467, \quad \phi_2 = 0{\cdot}2747, \tag{4.17}$$

and

$$\eta_i = e^{-\frac{1}{6}} \simeq 0{\cdot}8465.$$

Equation (4.16) generates a plausible curve which passes close to the data (see figures 2 and 3) and in fact also describes region II quite well [in the range $0{\cdot}5 < \eta < 1{\cdot}3$ (4.16) is within 1% of (3.1)]. Moreover, ϕ_0 is near the experimental value of 1·83 given by Hoffmann & Joubert. But (4.16) contains no direct n dependence and the general solution implies that it should be n dependent. In view of the close fit to the data, therefore, we must assume that the solution we have found is close to that for the case $n \simeq \frac{3}{4}$, although it is likely that the circulation distributions in regions I and II are, in any case, only weakly n dependent.

4.6. *Region III*

In region III we are, by definition, approaching the limit of the domain in which the rolled-up spiral of the vortex sheet can be treated as a continuum, and the spiral sheet here is still under the influence of the initial conditions imposed by the wing.

We should expect the actual solution for Φ_n^{III} to deviate slowly from Φ_n^{II} and ultimately merge with the asymptotic form for Φ in region III. But the data imply that the transition is somewhat abrupt [see figure 4(*b*)] and that the asymptotic form is reached almost immediately. Thus we could introduce a thin buffer layer to bridge the solution from region II to the asymptotic solution and this together with the asymptotic solution would approximate the actual solution in region III, and ensure continuity of circulation, vorticity etc. In doing so, however, we again suffer the problem of trying to force $\ln(\eta)$ to be analytically continuous, only this time to infinity rather than zero. In view of this and the rapid transition to the asymptotic form, we assume simply that the asymptotic solution for circulation is valid to η_s. This then defines our solution for region III. Thus from (2.2),

$$K^{\mathrm{III}}(\eta) \sim \phi_\infty^n \eta^{\frac{1}{2}(1-n)} \quad (\eta \to \infty), \tag{4.18}$$

where $\phi_\infty^n = (2\Gamma_\infty/N)\,(s/\alpha_n)^{n-1}$. And by matching (4.18) to (4.15) at $\eta = \eta_s$, we find

$$\tfrac{1}{2}\eta_s^{\frac{1}{2}(n-1)} \ln(e^2\eta_s) = \phi_\infty^n.$$

4.7. *The Reynolds-stress distribution*

Equations (4.15), (4.16) and (4.18) comprise a piecewise-continuous solution for $K(\eta)$, and thus $\Phi(\eta)$, for all η [$\eta^{-\frac{1}{2}}K(\eta)$ is plotted in figure 3 and $\Phi(\eta)$ in figure 5]; and in determining this solution no assumptions have been made regarding the nature of the turbulent shear stress. So, as the only unknown in (4.11) is the particular integral Φ_n^{I}

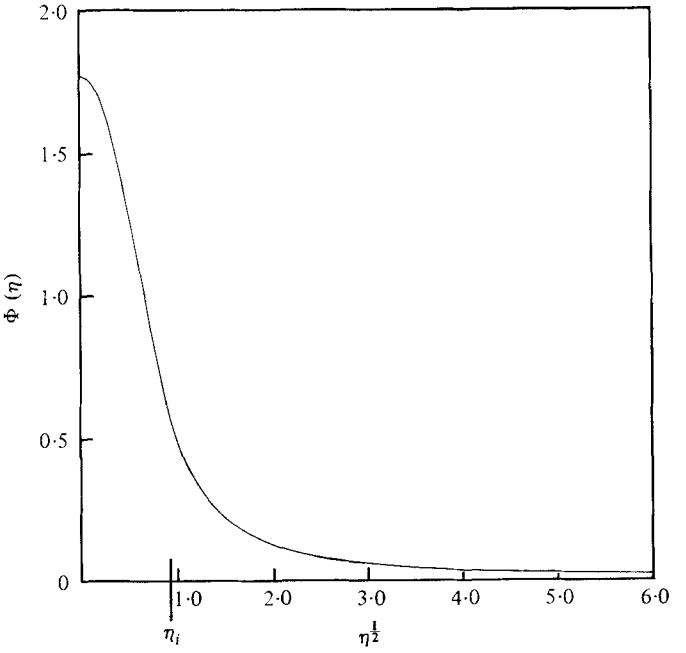

FIGURE 5. Distribution of the function $\Phi(\eta)$.

(which represents the Reynolds stress) we can now solve for it. In terms of $G_n(\eta)$ (see (4.4)), we find that, in region I (to second order),

$$G_n^{\mathrm{I}}(\eta) \simeq (\tfrac{1}{8}A_2\phi_0(1+n)-\phi_1)\,\eta+(-\tfrac{1}{12}A_2\phi_1(3+n)+2\phi_2)\,\eta^2+\frac{C_{12}}{\eta}+C_{11} \quad (0 \leqslant \eta \leqslant \eta_i); \quad (4.19)$$

in region II,

$$G_n^{\mathrm{II}}(\eta) \simeq \tfrac{1}{8}A_2(n-1)\,[\ln(\eta)-1]-\frac{\ln(\eta)}{2\eta}+\frac{C_{22}}{\eta}+C_{21} \quad (\eta_i \leqslant \eta \leqslant \eta_s); \quad (4.20)$$

and, in region III,

$$G_n^{\mathrm{III}}(\eta) \sim -\tfrac{1}{2}\phi_\infty^n(1+n)\,\eta^{(-n-1)/2}+\frac{C_{32}}{\eta}+C_{31} \quad (\eta_s \leqslant \eta < \infty); \quad (4.21)$$

where $C_{11} = C_{12} = C_{31} = 0$,

$$C_{21} = \frac{\ln(\eta_i)}{2\eta_i}-\tfrac{1}{8}A_2(n-1)\,[\ln(\eta_i)-1]+[\tfrac{1}{8}A_2\phi_0(1+n)-\phi_1]\,\eta_i + [-\tfrac{1}{12}A_2\phi_1(3+n)+2\phi_2)\,\eta_i^2-\frac{C_{22}}{\eta_i},$$

$$C_{22} = \tfrac{1}{8}A_2(n-1)\,\eta_i-\tfrac{1}{2}+\tfrac{1}{2}\ln(\eta_i)-[\tfrac{1}{8}A_2\phi_0(1+n)-\phi_1]\,\eta_i^2-[-\tfrac{1}{6}A_2\phi_1(3+n)+4\phi_2]\,\eta_i^3$$

and

$$C_{32} = \eta_s\left\{\tfrac{1}{8}A_2(n-1)\,[\ln(\eta_s)-1]-\frac{\ln(\eta_s)}{2\eta_s}+\tfrac{1}{2}\phi_\infty^n(1+n)\,\eta_s^{(-n-1)/2}+\frac{C_{22}}{\eta_s}+C_{21}\right\}.$$

Note here that, while the expressions for vorticity, circulation and tangential velocity in regions I and II are independent of n, the expressions for $G(\eta)$ are not.

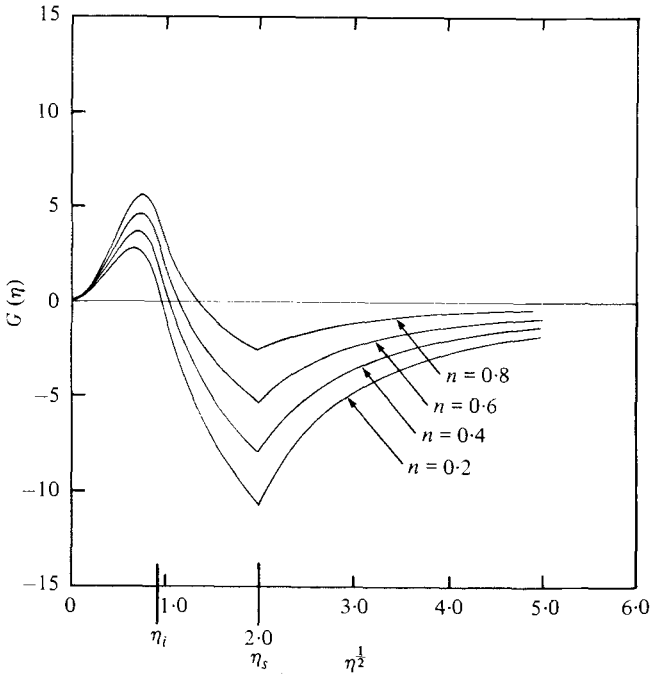

FIGURE 6. Variation of $G(\eta)$ with the parameter n: $A_2 = 50$; η_s assumed = 4·0.

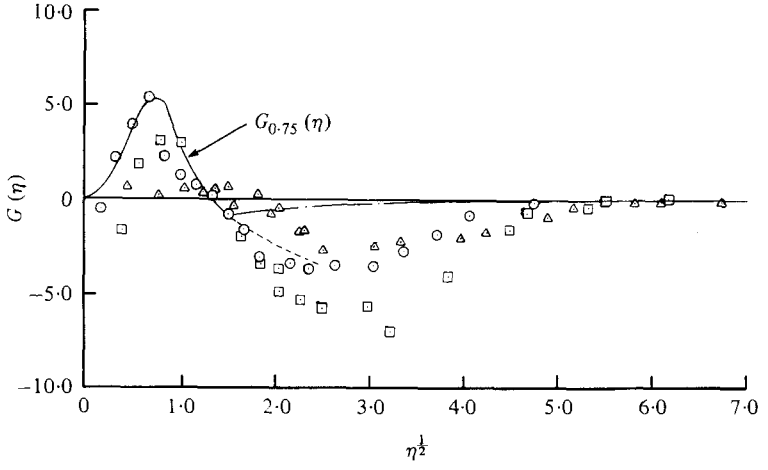

FIGURE 7. Comparison of $G_{0\cdot75}(\eta)$ with experimental data. Data of Graham & Phillips (1975) averaged over inward and outward traverse; ⊙, $z/c = 109$, case B; ⊡, $z/c = 109$, case C; △, $z/c = 109$, case D.

This means physically that, although the vorticity distribution may have reached a form virtually independent of initial conditions, the Reynolds stress has not. This is not unusual for developing self-preserving flows (see Wygnanski & Fiedler 1969).

The function $G_n(\eta)$ is plotted in figure 6 for values of n from 0·2 to 0·8 with $A_2 = 50$ and in figure 7 we compare the $\overline{v'w'}$ data of Graham & Phillips (1975) with $G_{0\cdot75}(\eta)$

and $A_2 = 50$. The distribution of Reynolds stress is close to what was anticipated in § 3.4.

5. Reynolds-number dependence?

According to the principle of Reynolds-number similarity in free turbulent shear flows, the motion of the large-scale (energy-containing) eddies is essentially inviscid, and so independent of Reynolds number (Townsend 1976). This means that the eddy viscosity, if suitably non-dimensionalized, must be independent of Reynolds number and hence time and distance downstream, although of course it may vary in the cross-stream direction.

The turbulent trailing vortex data summarized by Owen (1970), however, indicate that the eddy viscosity (defined by him as $r_1^2/4t$) varies by two orders of magnitude over the Reynolds-number range 10^3 to 10^7, implying either a fallacy in the foregoing reasoning, or (as seems more likely) an inappropriate expression for the eddy viscosity. Having determined the distribution of Reynolds stress throughout the vortex, we are now in a position to determine the approximate form of the eddy viscosity; this may then provide, at least, a partial explanation for its apparent dependence on Reynolds number.

Following the convention of replacing ν, the molecular viscosity, by ν_e, an apparent one, we find

$$\frac{\nu_e}{\nu} = 1 - G_n(\eta) \Big/ \eta \frac{d}{d\eta}\left(\frac{K}{\eta}\right). \tag{5.1}$$

The right-hand side of (5.1) is independent of time, implying that ν_e is a function of η only; it is also independent of ν, implying that the eddy viscosity is independent of Reynolds number. Both results are compatible with the principle of Reynolds-number similarity. Furthermore, the distribution of ν_e/ν is dependent upon the initial conditions n and A_2 [via $G(\eta)$]. Now the physical meaning of n is clear, but what does A_2 represent? We know that A_2 is a dimensionless constant ($= r_1^2/2\nu t$) and that with an equilibrium structure $A_2 \gg 1$. Moreover $\frac{1}{2}\nu A_2$ is what Owen called the eddy viscosity and it is this parameter which varies with Reynolds number, but why?

To provide a partial answer to this question, consider the shedding process from the wing and recall that the order of the thickness of the trailing-vortex layer is initially that of the boundary layer at the wing trailing edge. So the size of the initial vortex core which forms, and in consequence sets A_2, depends strongly upon δ near the tip of the wing. As δ is affected by Reynolds number (and other parameters such as wing plan form, twist and loading etc.) it must finally be reflected in the value of A_2; hence the apparent dependence on Reynolds number.

We may conclude, therefore, that the turbulent trailing vortex does conform to the principle of Reynolds number similarity for free turbulent shear flows and, moreover, that Reynolds number effects are reflected in the parameter A_2. We may also note that accurate *a priori* determination of A_2 appears somewhat difficult, although, as we shall see in § 6, it may readily be determined experimentally.

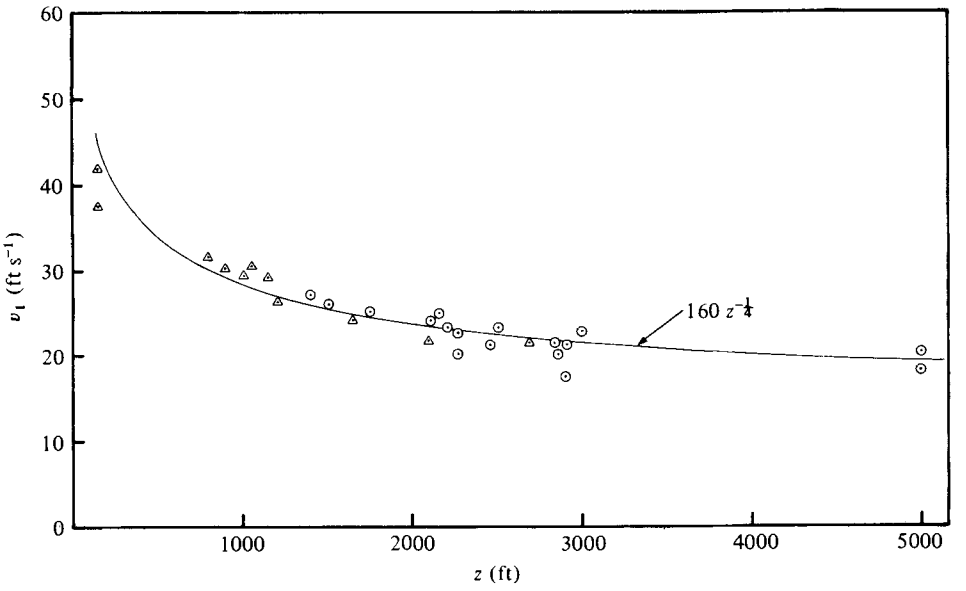

FIGURE 8. Downstream variation of peak tangential velocity. Data of McCormick *et al.* (1968): ⊙, Army O-1 aircraft; △, Cherokee aircraft. $U_\infty = 132$ ft s^{-1}. ——, present theory.

6. Discussion

In §4.1 we assumed that both A_1 and A_2 are positive, and, while it is clear that A_2 must be positive (if r_1 is increasing with time), the sign of A_1 is not nearly as obvious. With both constants positive, the resulting growth rates are $r_1 \propto t^{\frac{1}{2}}$ and

$$v_1 \propto t^{-\frac{1}{2}n}. \tag{6.1}$$

Thus for a delta wing, where n is only slightly greater than zero, we see that v_1 will decay very slowly. On the other hand, with $A_1 < 0$ and $A_2 > 0$, then $A_1/A_2 = n-1$, yielding

$$v_1 \propto t^{\frac{1}{2}(n-2)}. \tag{6.2}$$

For the same delta wing, (6.2) indicates that v_1 would decay almost inversely with time, and the data of Bisgood, Maltby & Dee (1971) support the latter. With $A_1 < 0$, however, we cannot satisfy the assumption that ζ is invariant with time; indeed, if A_1 is negative, then ζ must vary with time, like t^{n-1}. But, with $A_1 > 0$, we do satisfy the assumption on ζ. This presents an apparent anomaly, and in answer we suggest the following.

In the early stages of roll-up, when the two vortices are small compared with the wing span ($r_1 \ll \frac{1}{2}s$) and their influence upon each other is negligible, ζ must be independent of time. In this situation, the theory can be valid only if $A_1 > 0$. Some distance downstream, however, where the vortices are no longer small compared with the wing span, their influence upon each other can cause ζ to be time dependent; although it is not obvious that its dependence will be of the form t^{n-1}. With this supposition, the theory is then valid only if $A_1 < 0$.

We suggest therefore that there can be two modes of decay in a rolling-up turbulent

trailing vortex: in the first mode $r_1 \ll \frac{1}{2}s$ and v_1 decays like $t^{-\frac{1}{2}n}$; and, in the second mode, $r_1 = O(\frac{1}{2}s)$ and v_1 decays (perhaps) like $t^{\frac{1}{2}(n-2)}$. Two modes of decay are in fact hinted at by Bisgood *et al.* who suggest that their delta wing data imply that v_1 asymptotes to t^{-1} only after some time (about forty spans behind the wing).

Now if the decay remains in mode 1 for most of the roll-up (something not unreasonable to expect behind a high-aspect-ratio rectangular wing), (6.1) suggests that for large time (for any n, $0 < n < 1$) a plateau region of very slow decay will result. This plateau region was first inferred from McCormick, Tangler & Sherrieb's (1968) data by Nielsen & Schwind (1971). We plot this data in figure 8 and scribe onto it (6.1) assuming $n = 0{\cdot}5$ (elliptic loading).† The agreement is encouraging, but it is questionable to use a constant value of n over such a time scale.

The simplicity of a single parameter n to describe the form of the rolling-up vortex sheet is attractive in an analysis such as the present but, as Moore points out, Kaden's model overpredicts the roll-up rate once about half of the sheet's vorticity is contained within the spiral. For the latter part of the rolling-up process then, n must become a weak function of time, rendering the analysis valid only in the quasi-steady sense. This is perhaps not surprising physically, as the vortex sheet, with time, must eventually forget the initial conditions which led to its development, although, for practical purposes, the error introduced by assuming n to remain constant is probably no greater than the error arising from the uncertainty in the value of A_2.

I am indebted to Dr M. R. Head and Professor D. W. Moore for their many helpful suggestions during the preparation of this paper. This work was supported by Rolls Royce (1971) Ltd.

Appendix. Saffman's theorem and overcirculation during roll-up

Writing $\partial\Gamma/\partial t$ as $\partial(\Gamma - \Gamma_\infty)/\partial t$, substituting into (4.1), integrating with respect to r between O and a_0 and then with respect to t, we obtain, after dividing throughout by r_1^2,

$$\frac{\Gamma_\infty}{\Gamma_0(t)} \int_0^{\eta_0(t)} \frac{(\Gamma_\infty - \Gamma)}{2\Gamma_\infty} \mathrm{d}\eta = \frac{\nu(1+n)^2 t}{2r_1^2} + \frac{2\pi \int \vartheta(t)\, dt}{\Gamma_0 r_1^2} + \frac{A_3}{r_1^2}, \tag{A 1}$$

where $\Gamma_0 = 2\pi\zeta a_0^{1-n}$ and A_3 is a dimensional constant.

For the fully rolled-up vortex $a_0 \to \infty$, $\Gamma_0 \to \Gamma_\infty$ and $\vartheta = 0$; moreover, if r_1 is growing faster than $(\nu t)^{\frac{1}{2}}$ then the right-hand side is decreasing, implying that at large time, $\Gamma > \Gamma_\infty$ over some η (Govindaraju & Saffman 1971). For the rolling-up case, r_1 is not growing faster than $(\nu t)^{\frac{1}{2}}$. Substituting for r_1, the right-hand side of (A 1) becomes

$$\frac{(1+n)^2}{4A_2} + \frac{2\pi \int \vartheta(t)\, dt}{\Gamma_0 2\nu A_2 t} + \frac{A_3}{2\nu A_2 t}. \tag{A 2}$$

Since $A_2 \gg 1$, we can ignore the first term and if ϑ is independent of time the second term becomes a constant equal to $\pi\vartheta/\Gamma_0\nu A_2$ ($= \pi B$, say).

Now for overcirculation to occur the sum of (A 2) must be less than $\frac{1}{6}$, so (noting

† At 2500 feet downstream, McCormick *et al.* give $v_1 \simeq 22$ ft s^{-1} and $r_1 \simeq 5$ ft ($U_\infty = 132$ ft s^{-1}); therefore $A_2 = 4125$ (from (4.12)) and as $v_1 = \text{constant} \times r_1^{-n}$ (from (6.1)), we see that $v_1 \simeq 160\, z^{-\frac{1}{4}}$.

that there can also be a contribution from the third term if $A_3 \neq 0$) overcirculation is excluded providing $B \geqslant 1/6\pi$ or G is $\geqslant \frac{1}{6}A_2K(\eta)\eta^{-1}$.

As the data given in figure 7 suggests strongly that G does equal, or exceed,

$$\tfrac{1}{6}A_2K(\eta)\eta^{-1} \quad \text{as} \quad \eta \to \eta_0 \quad (\text{for } A_2 \simeq 50 \quad \text{and} \quad K(\eta) \simeq 1),$$

it would seem that overcirculation is most unlikely during the roll-up process.

REFERENCES

BATCHELOR, G. K. 1964 *J. Fluid Mech.* **20**, 645–658.

BISGOOD, P. L., MALTBY, R. L. & DEE, F. W. 1971 *Aircraft Wake Turbulence and its Detection*, pp. 171–206. Plenum.

FAGE, A. & SIMMONS, L. F. G. 1925 *Phil. Trans. Roy. Soc* A **225**, pp. 303–326.

FINK, P. T. & SOH, W. K. 1978 *Proc. Roy. Soc.* A **362**, 195–209.

GOVINDARAJU, S. P. & SAFFMAN, P. G. 1971 *Phys. Fluids* **14**, 2074–2080.

GRAHAM, J. A. H., NEWMAN, B. G. & PHILLIPS, W. R. C. 1974 *Proc. 9th Cong. Int. Counc. Aero. Sci.* no. 74–40.

GRAHAM, J. A. H. & PHILLIPS, W. R. C. 1975 *McGill Univ.* MERL TN 75–1.

HILTON, W. F. 1938 *Aero. Res. Counc. R. & M.* 1858.

HOFFMANN, E. R. & JOUBERT, P. N. 1963 *J. Fluid Mech.* **16**, 395–411.

KADEN, H. 1931 *Ing. Arch.* **2**, 140–168.

LEIBOVICH, S. 1978 *Ann. Rev. Fluid Mech.* **10**, 221–246.

MASKELL, E. C. 1962 *Proc. 3rd Cong. Int. Counc. Aero. Sci.*, pp. 737–750.

MASON, W. H. & MARCHMAN, J. F. 1972 *N.A.S.A.* CR 62078.

MCCORMICK, B. W., TANGLER, J. L. & SHERRIEB, H. E. 1968 *J. Aircraft* **5**, 260–267.

MOORE, D. W. 1974 *J. Fluid Mech.* **63**, 225–235.

MOORE, D. W. & SAFFMAN, P. G. 1973 *Proc. Roy. Soc.* A **333**, 491–508.

NIELSEN, J. N. & SCHWIND, R. G. 1971 *Aircraft Wake Turbulence and its Detection*, pp. 413–454. Plenum.

OWEN, P. R. 1970 *Aeronaut. Q.* **21**, 69–78.

PULLIN, D. I. & PHILLIPS, W. R. C. 1981 *J. Fluid Mech.* **104**, 45–53.

SAFFMAN, P. G. 1973 *Phys. Fluids* **16**, 1181–1188.

SLATER, L. J. 1960 *Confluent Hypergeometric Functions.* Cambridge University Press.

SQUIRE, H. B. 1965 *Aeronaut. Q.* **16**, 302–306.

TOWNSEND, A. A. 1976 *The Structure of Turbulent Shear Flow*, 2nd edn. Cambridge University Press.

WIDNALL, S. E. 1975 *Ann. Rev. Fluid Mech.* **7**, 141–166.

WYGNANSKI, I. & FIEDLER, H. E. 1969 *J. Fluid Mech.* **38**, 577–612.